

1 **Two waves of evolution in the rodent pregnancy-specific glycoprotein**
2 **(PSG) gene family lead to structurally diverse PSGs**

3

4

Robert Kammerer^{1*}, Wolfgang Zimmermann^{2,3}

5

6 ¹Institute of Immunology, Friedrich-Loeffler Institute, Greifswald-Insel Riems, Germany

7 ²Tumor Immunology Laboratory, LIFE Center, LMU Klinikum, University Munich, Germany

8 ³Department of Urology, LMU Klinikum, University Munich, Germany

9

10

11 Correspondence: *Robert.Kammerer@fli.de

12

13 WZ: Wolfgang.Zimmermann@med.uni-muenchen.de

14

15 Short title: Evolution of Pregnancy-specific glycoproteins in rodents

16

17 Keywords

18 pregnancy-specific glycoprotein (PSG); Carcinoembryonic antigen (CEA); carcinoembryonic antigen-

19 related cell-cell adhesion molecule (CEACAM); immunoglobulin superfamily; rodents; trophoblast;

20 hemochorial placenta.

21

22 **ABSTRACT**

23 The evolution of pregnancy-specific glycoproteins (PSGs) within the CEA gene family of primates
24 correlates with the evolution of hemochorial placentation about 45 Myr ago. Thus, we
25 hypothesized that hemochorial placentation with intimate contact between fetal cells and
26 maternal immune cells favors the evolution and expansion of PSGs. With only a few exceptions,
27 all rodents have hemochorial placentas thus the question arises whether PSGs evolved in most
28 rodent genera.

29 Analyzing genomic data of 94 rodent species we could identify PSGs only in three families of the
30 suborder Myomorpha (characteristic species in brackets) namely in the Muridae (mouse),
31 Cricetidae (hamster) and Nesomyidae (giant pouched rat) families. No PSGs were detected in the
32 suborders Anomaluomorpha (springhare), Castorimorpha (beaver), Hystricognatha (guinea pig)
33 and Sciuromorpha (squirrel). Thus, PSGs evolved only recently in Myomorpha shortly upon their
34 most recent common ancestor (MRCA) has coopted the retroviral genes syncytin-A and syncytin-B
35 which enabled the evolution of the three-layered trophoblast. This may suggest that the evolution
36 of *Psgs* in rodents may have been favored by the challenge of the newly invented architecture of
37 the maternal-fetal interface. In addition, a second hallmark of rodent PSG evolution seems to be
38 the translocation of genes from the CEA gene family locus into a unique genomic region. Rodents
39 without PSGs do not have any CEA-related genes in this locus. In contrast, rodent species in which
40 PSGs evolved have lost ITAM-encoding CEACAM genes indicating that such a gene was
41 translocated and thereby destroyed to form the new rodent PSG locus. This locus contains at least
42 one *Psg* and *Ceacam9* indicating that one of them was the founder gene of rodent *Psgs*. These
43 genes are composed of various numbers of IgV-like domains (N domains) and one carboxy-
44 terminal IgC-like domain of the A2-type. In a second wave of gene amplification in the PSG locus
45 a gene encoding a protein composed of two N domain gave rise to four genes in mice (*Ceacam11-14*).
46 In light of the divergent structure of PSGs in various mammalian species, we hypothesized
47 that the *Ceacam11-14* encode also functional PSGs and indeed we found that they are
48 preferentially expressed by spongiotrophoblast cells, like *Psg* genes.

49

50

51

52

53 **Background**

54 Pregnancy-specific glycoproteins (PSGs) were first described in humans as proteins in the serum
55 of pregnant women [1]. Subsequently, the genes which encode human PSGs were identified and
56 found to be members of the carcinoembryonic antigen (CEA) gene family which by itself is a
57 member of the immunoglobulin gene superfamily [2, 3]. Once the CEA gene families were
58 investigated in mice and rats a subgroup of the gene products was identified as secreted
59 glycoproteins that were predominantly expressed by trophoblast cells and were named as PSGs
60 in rodents [4-6]. Surprisingly, the structure of rodent PSGs differs significantly from that of human
61 PSGs [6]. While human PSGs are composed of one N terminal immunoglobulin variable (IgV)-like
62 domain (also called, N domain) and two to three immunoglobulin constant (IgC)-like domains
63 (two A and one B domains) murine PSGs contain three to eight N domains followed by a single
64 IgC domain of the A2-type found among others in CEACAM1 [7]. This led to the assumption that
65 primate and rodent PSGs evolved independently in both orders. More recently, we found that in
66 some microbat species, putative PSGs exist, composed of a single N domain followed by a single
67 A domain [8]. Furthermore, in horses PSGs consisting of a single N domain were identified [9].
68 Despite the vast structural differences, common functions were described for PSGs of different
69 species such as inhibition of platelet aggregation, activation of latent TGF β and other immune-
70 modulating functions [9-13] suggesting that PSGs developed independently in different
71 mammalian lineages by convergent evolution [14]. This raises the question about the driving force
72 of PSG evolution within the CEA gene family. Based on the fact that humans, mice, and rats as
73 well as the above-indicated bat species have a hemochorial placenta, where fetal trophoblast
74 cells have direct contact with maternal immune cells we and others hypothesized that PSGs
75 evolved to regulate maternal immunity against fetal antigens [15, 16]. Indeed, it was found that
76 equine PSGs were expressed by highly invasive trophoblast cells the so-called girdle cells which
77 later form endometrial cups, a unique structure in equine placenta [9]. It is well documented that
78 these cells are recognized by the maternal immune system which is also expected for trophoblast
79 cells in mammals with hemochorial placentation [17]. Furthermore, in primates PSGs were found
80 only in species with hemochorial placentas but not in primates that have an epitheliochorial
81 placenta further pointing to an association of PSG evolution and intimate interaction of fetal
82 trophoblast cells and the maternal immune cells [16]. Rodents, with only very few exceptions,
83 have a hemochorial placenta, so we wondered when the PSGs evolved in rodents [18]. Rodents
84 first appear in the fossil record at the end of the Paleocene and earliest Eocene, about 54 million
85 years ago (Mya) [19]. Nowadays, the order Rodentia comprises about 40 % of all mammalian
86 species [20] and is divided into five suborders, the Anomaluomorpha (e.g. springhares),
87 Castorimorpha (e.g. beavers and kangaroo rats), Myomorpha (e.g. mice and hamsters),
88 Hystricomorpha (e.g. guinea pigs and chinchillas) and the Sciuromorpha (e.g. squirrels and
89 mountain beavers) [21]. Mice and Rats belong to the Myomorpha suborder which appeared ~26
90 mya. The *Mus-Rattus* split is estimated to have occurred 8.8 to 10.3 mya ago [22]. Since PSGs in
91 mice and rats are thought to have a common ancestor this indicates that PSGs in rodents evolved

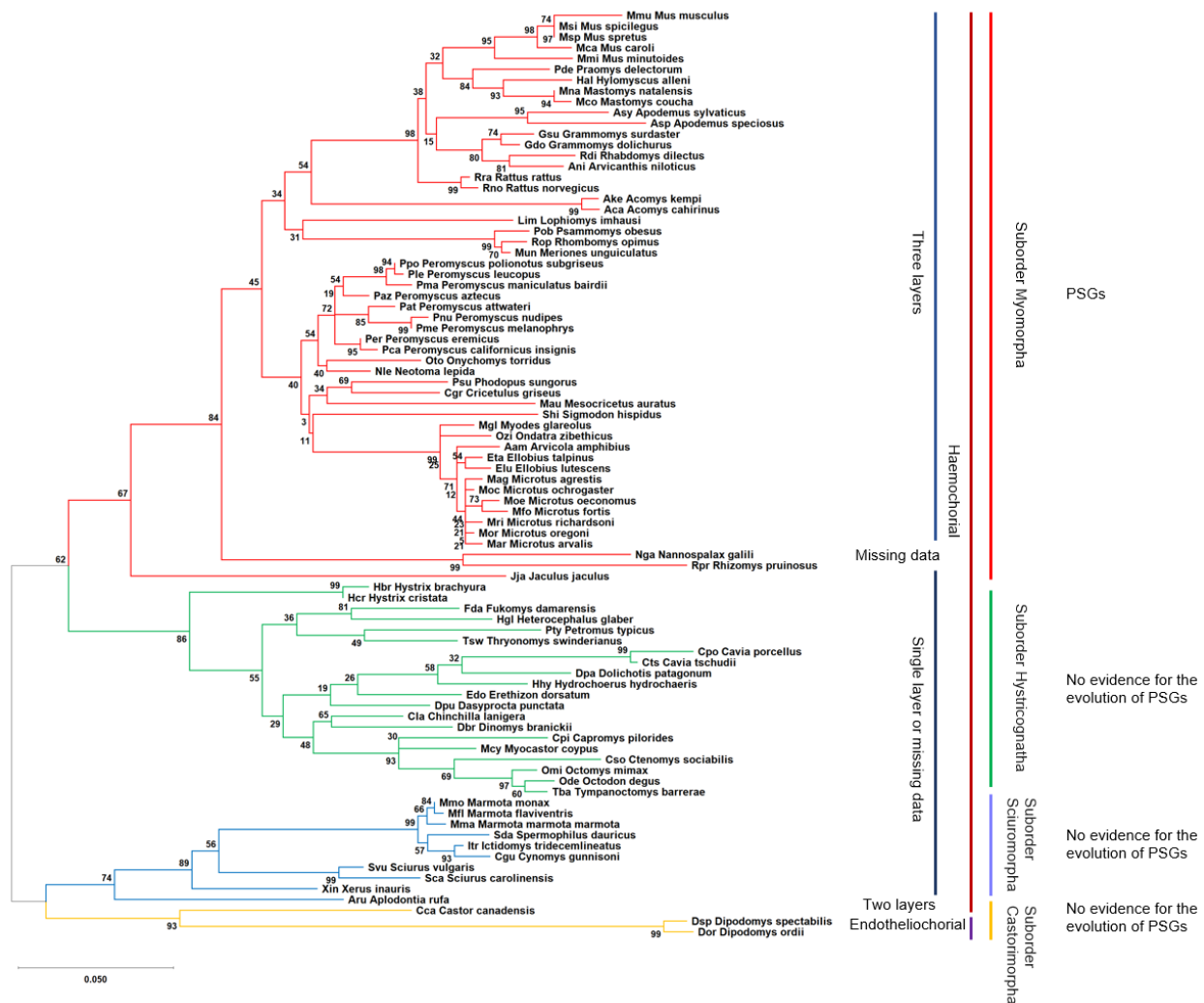
92 at least about 10 mya ago. But what happened during the remaining 40 million years of rodent
93 existence? To answer this question, we investigated the CEA gene families in 94 rodent species
94 containing members of the rodent suborders Myomorpha, Hystricomorpha, Sciuromorpha, and
95 Castorimorpha. We found only supporting evidence for the evolution of PSGs in Muroidea, a
96 subgroup of the Myomorpha, not in other rodents. The key event for the amplification of PSGs
97 was most likely the translocation of CEA gene family member(s) or parts of them from the CEA
98 gene family locus into the *Npas1/Pglyrp1* locus. In this locus three, structurally different members
99 of the CEA gene family could be found which all encode secreted glycoproteins. PSGs consists of
100 multiple N domains and a single A domain, Ceacam11-14 consists of two N domains, and Ceacam9
101 and Ceacam15 are composed of one N domain and one A domain. According to their expression
102 pattern in mice, all of them have to be considered to be functional PSGs. Thus, domain
103 arrangements of PSGs do not only differ fundamentally between species but also within a single
104 species.

105

106 **Results**

107 **Recent evolution of pregnancy-specific glycoproteins in rodents**

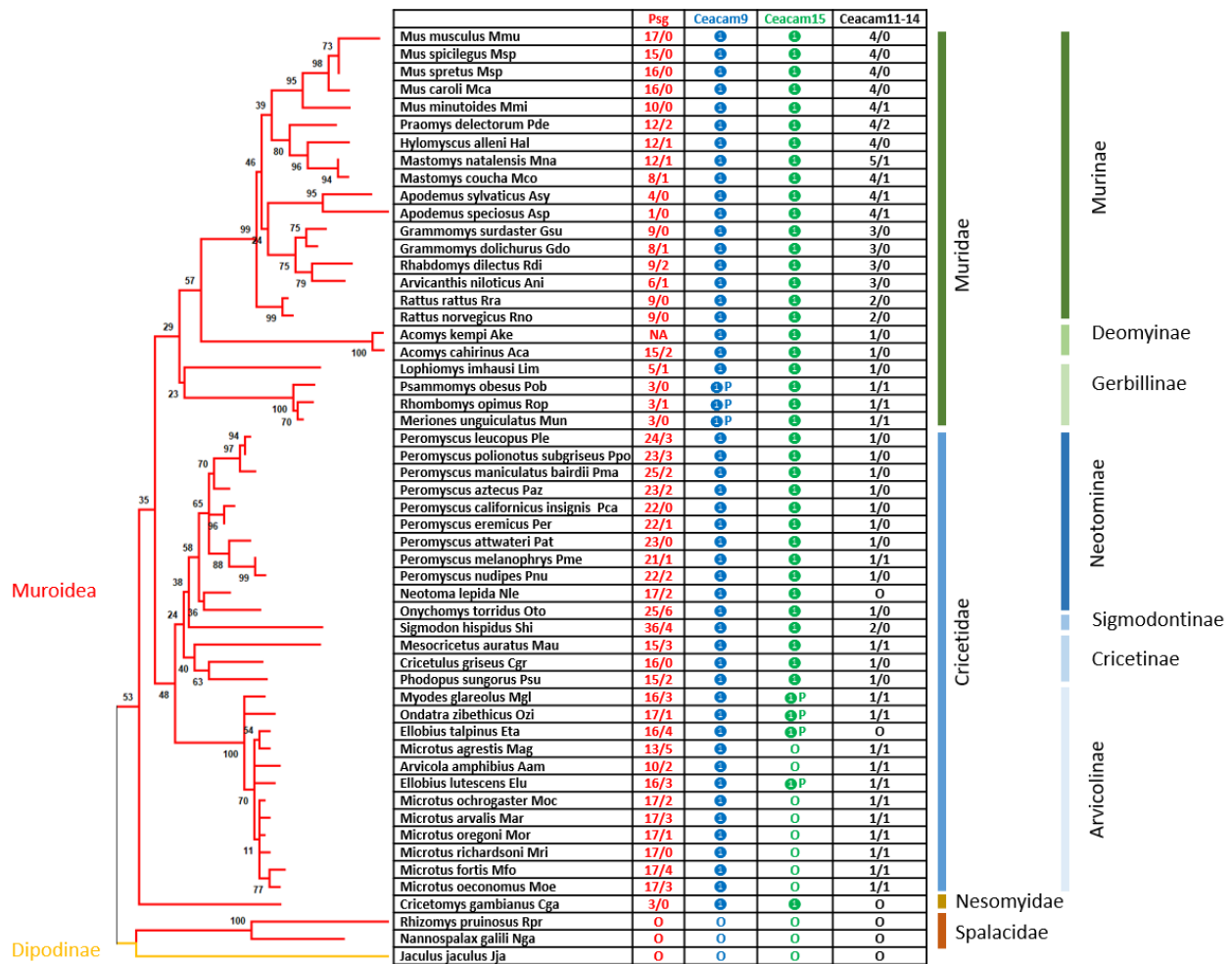
108 *Psgs* are well described for mice and rats but so far not for other rodents. In mice and rats, *Psgs*
109 are located in the genome locus flanked by marker genes *Npas1* and *Pglyrp1* [23]. This locus will
110 be further referred to as the “rodent *Psg* locus” in this publication. In contrast, no CEA gene family
111 members are present in this region in primate genomes [16]. In mice, in addition to the 17 *Psgs*
112 (*Psg16-Psg32*) *Ceacam9* and *Ceacam11-15* are located at this locus [7, 24]. To get first insights
113 into the evolution of *Psgs* in rodents, other than mice and rats, we used the sequences of the
114 above-mentioned mouse genes to identify *Psgs* in the genome of 94 rodent species using the
115 Basic Local Alignment Search Tool (BLAST) and the NCBI and Ensemble databases (Fig. 1,
116 Supplementary Table 1). *Psgs*, composed of three or more N domains and one IgC-like domain as
117 described for mice and rats, were identified only in the suborder Myomorpha but not in the
118 suborders Castorimorpha, Hystricomorpha and Sciuromorpha (Fig. 1).



119
 120 **Figure 1. Phylogeny of the analyzed rodent species.** The phylogenetic tree was constructed using
 121 the N domain exon nucleotide sequences from *Cecam19* genes. The color of the branches
 122 indicates the suborder to which the species belong. The type of placenta is indicated on the right.
 123 The presence of *Psg* genes is indicated.

124
 125 *Psgs* were found in all analyzed species of the suborder Myomorpha except in the genome of the
 126 lesser Egyptian jerboa (*Jaculus jaculus*; Dipoditae) and the two members of the Spalacidae family
 127 the Upper Galilee mountains blind mole rat (*Nannospalax galili*) and the hoary bamboo rat
 128 (*Rhizomys pruinosus*) (Fig. 2). Thus, the presence of *Psgs* is limited to three rodent families
 129 (Cricetidae, Muridae and Nesomyidae) of the Muroidea clade. Interestingly, the number of *Psgs*
 130 varied widely from three genes in the genome of the African giant pouch rat (*Cricetomys*
 131 *gambianus*) a member of the Nesomyidae family and of the Mongolian gerbil (*Meriones*
 132 *unguiculatus*), the great gerbil (*Rhombomys opimus*) and the fat sand rat (*Psammomys obesus*)
 133 all three are members of the Gerbillinae subfamily, to 25 genes (including 2 pseudogenes) in the
 134 North American deer mouse (*Peromyscus maniculatus*; Neotominae subfamily) (Fig. 2).
 135 Interestingly, in all rodent species where we identified *Psgs* we also identified *Cecam9* orthologs,

136 although in the three Gerbillinae species (*Meriones unguiculatus*, *Rhombomys opimus*,
 137 *Psammomys obesus*) *Ceacam9* seem to be a pseudogene due to a common two nucleotide
 138 deletion in the N domain exon (Fig. 2). *Ceacam15* orthologs were found in all species which have
 139 *Psgs* and *Ceacam9* except in species of the Arvicolinae subfamily (Fig. 1, Fig. 2). However, a
 140 possible remnant of *Ceacam15* was found in the two Ellobius species as well as in the genome of
 141 *M. glareolus* and *O. zibethicus*, indicating that *Ceacam15* was lost in the Arvicolinae subfamily. In
 142 species that do not have *Psg* genes, neither *Ceacam9* orthologs nor *Ceacam15* orthologs were
 143 found (Fig. 2). Genes related to murine *Ceacam11-14* are found in a subgroup of the species with
 144 *Psgs* and are described in more detail below.
 145



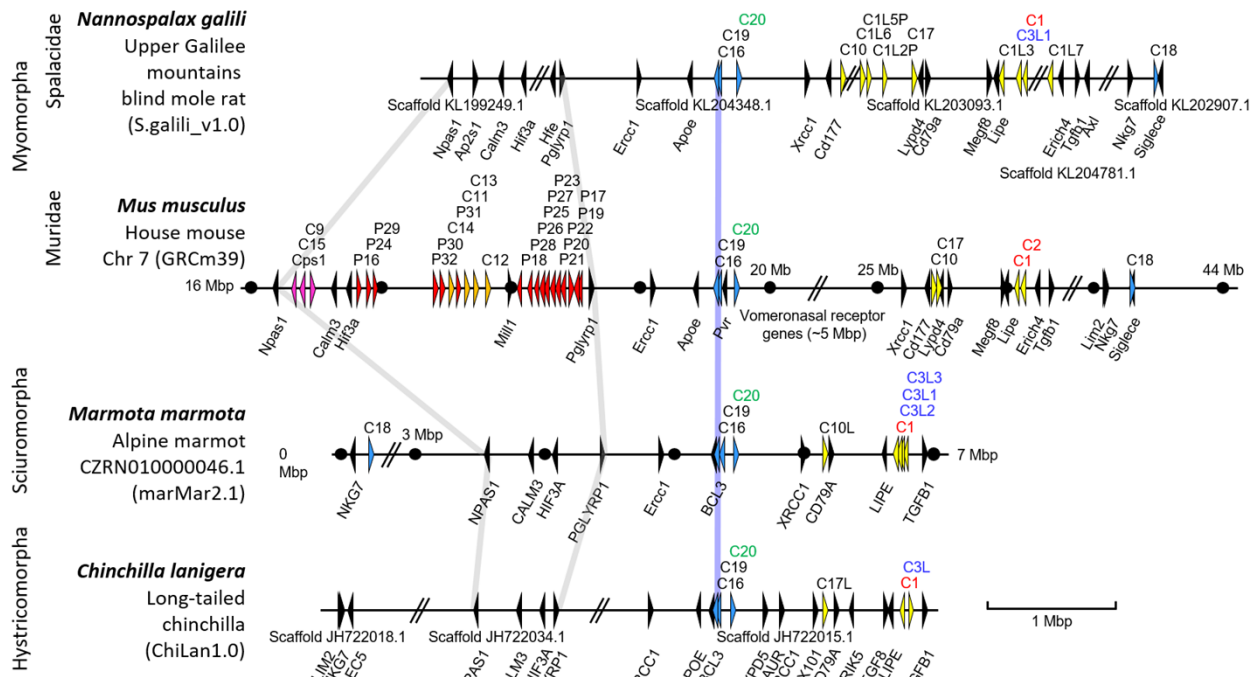
146
 147 **Figure 2. PSGs evolved in the clade Muroidea.** The phylogenetic tree was constructed with the
 148 nucleotide sequences of the *Ceacam19* N domain exons. Genes found in the genome locus
 149 flanked by marker genes *Npas1* and *Pglyrp1* were analysed in 54 species of the suborder
 150 Myomorpha. Open circles indicate that the gene was not found in the genome; filled circles
 151 specify that the gene was identified in the genome as a single copy; P next to the filled circle
 152 indicates that the gene is a pseudogene according to our definition (Material and Methods). NA

153 = not analysed; The numbers indicate the total number of genes identified/the number of genes
 154 expected to represent pseudogenes.

155
 156 **Coincidence of *Psg* appearance at the “rodent *Psg* locus” and loss of ITAM-encoding *Ceacams***
 157 **in rodent *CEA* gene families.**

158 In order to get further information about the possible origin of *Ceacam*-related genes at the
 159 rodent *Psg* locus we analysed the chromosomal arrangement of *Ceacam*-related genes. The
 160 analyses were restricted to species for which available scaffolds were long enough to cover the
 161 entire *Ceacam/Psg* locus. Selected species are depicted in Fig. 3. Remarkably, species which lack
 162 *Psgs* do also not harbor any other members of the *Cea* gene family in the “rodent *Psg* locus” (Fig.
 163 3). This was verified for species belonging to the Suborders Hystricomorpha and Sciuromorpha as
 164 well as to the members of the Spalacidae family (Fig. 3). This may indicate that a single
 165 translocation of one or more *Cea* gene family members gave rise to the evolution of all *Cea* gene
 166 family members in the “rodent *Psg* locus”. However, in the *Ceacam* locus diverse differences and
 167 copy number variations could be observed. Interestingly, we observed that rodent species which
 168 do not have *Cea* gene family members in the “rodent *Psg* locus” have *Cea* gene family members
 169 encoding *Ceacams* which have activating signaling motifs in the cytoplasmic tails
 170 (Supplementary file 1). Of note such *Ceacams* were not found in rodent species in which *Psgs*
 171 evolved including mice and rats. In some species e.g. the alpine marmot (*Marmota marmota*)
 172 such genes even have been multiplied (Fig. 3, Supplementary file 1). This may tempt to speculate
 173 that an activating *Ceacam* was destroyed and subsequently lost due to the translocation of a
 174 *Ceacam* gene to form the “rodent *Psg* locus” in the MRA of *Psg* harboring rodents.

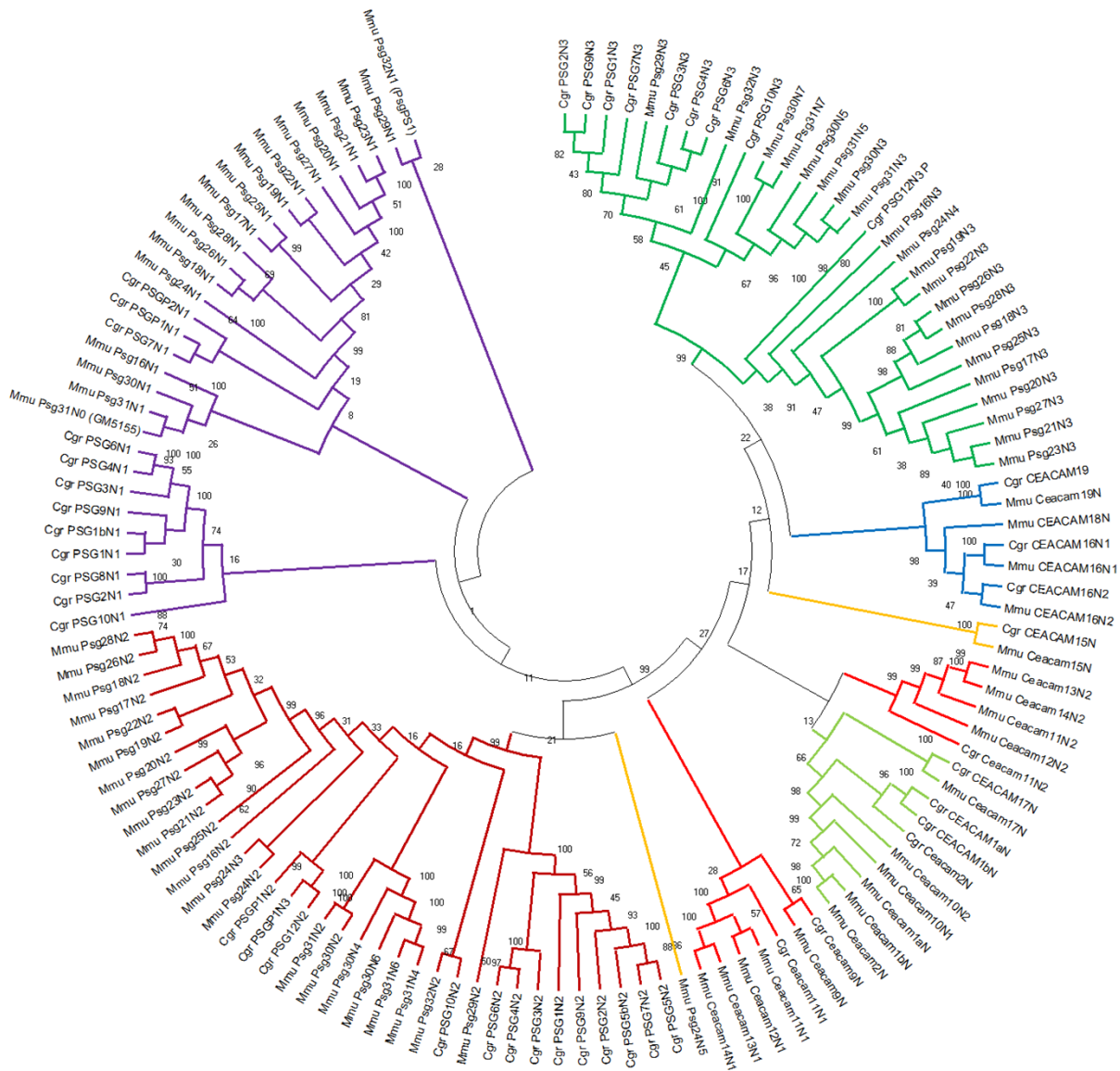
175



176

177 **Figure 3. Evolution of *Psgs* in rodents is restricted to the *Npas1/Pglyrp1* locus.** The chromosomal
178 arrangements of *Ceacam*-related genes of selected species of the Myomorpha (*Nannospalax*
179 *galili*, *Mus musculus*), Sciuromorpha (*Marmota marmota*), and Hystricomorpha (*Chinchilla*
180 *lanigera*) suborders are shown. Arrowheads indicate genes with their transcriptional orientation.
181 The *Psg*-related genes are shown in red (*Psg*), purple (*Ceacam9*, *Ceacam15*, and *Ceacam*
182 pseudogene 1, *Cps1*) or orange (*Ceacam11-14*), *Ceacam1*-related *Ceacam* genes in yellow,
183 conserved *Ceacam* genes in blue and selected flanking genes in black. The *Ceacam* gene loci were
184 aligned along the position of *Ceacam16* (blue line). Gray lines were used to delineate the
185 *Npas1/Pglyrp1* loci. Abbreviated names of *Ceacam1*-like genes with ITIM/ITSM-encoding exons
186 are shown in red and with ITAM and ITAM-like motif-encoding exons in green and blue,
187 respectively. Nucleotide numbering of the chromosomes starts at the telomere. Selected
188 positions 1 Mbp apart are indicated by dots. Databases and their versions used are listed below
189 the species name. The borders of scaffolds are indicated by double slashes, their names below
190 the chromosome. The exact distances between the scaffolds still have to be determined by
191 complete whole genome sequencing. Of note: The rodent genomes (except the murine genome)
192 are not completely sequenced yet. Therefore, not all *Ceacam* genes identified in whole genome
193 shotgun (WGS) databases have been found in the published assembled genomes. C, *Ceacam*; Cps,
194 *Ceacam* pseudogene; C1L1(P), *Ceacam1*-like (pseudo)gene, the same abbreviation schema
195 applies to similar abbreviations; Mbp, million base pairs; P, pregnancy-specific glycoprotein (*Psg*)
196 genes.

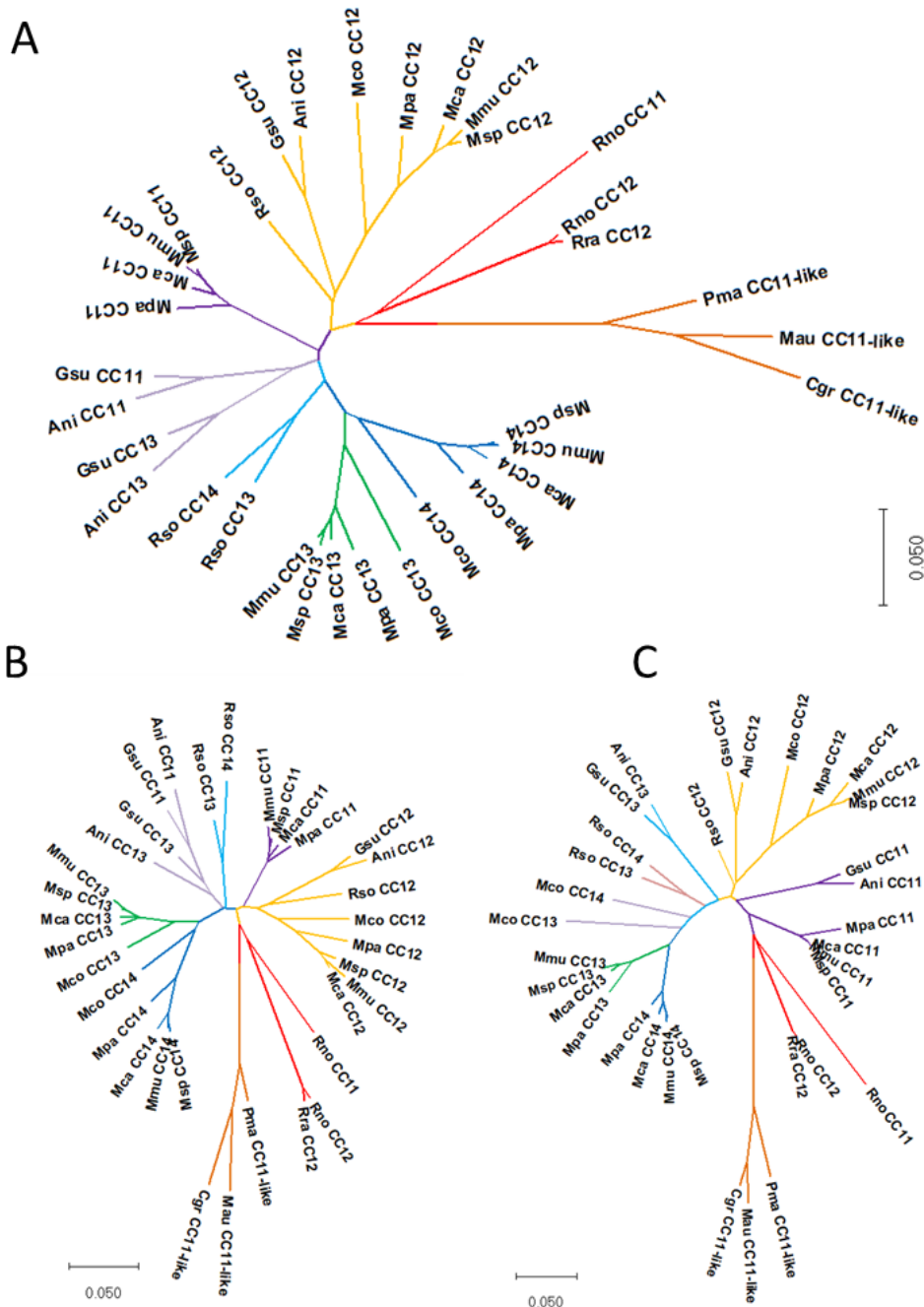
197
198 **A second wave of gene amplification led to the generation of murine *Ceacam11-14* genes.**
199 To further delineate the evolution of the *Ceacam*-related genes at the “rodent *Psg* locus” we
200 performed phylogenetic analyses of N domain exons of members of different muroid families i.e.
201 house mouse and Chinese hamster, using their nucleotide sequences. An orthologous
202 relationship was found for *Ceacam9*, *Ceacam15*, *Ceacam16*, *Ceacam17* and *Ceacam19* (Fig. 4).
203 Furthermore, mouse *Ceacam1*, *Ceacam2* and *Ceacam10N1* are closely related with *Ceacam1* and
204 *Ceacam2* in the Chinese hamster (*Cricetulus griseus*) but did not exhibit pairwise orthology. For
205 *Psgs* the N1 domain exon sequences build a cluster but no orthologous relationship between
206 individual *Psgs* of the two species could be identified. The N2 and N3-6 N domains did not
207 segregate completely into individual clusters indicating that recent exon duplication and shuffling
208 has taken place during expansion of *Psgs*. Remarkably, in the consensus tree the *Ceacam9* N
209 domain exon is closely related to the N1 domain exons of *Ceacam11-14* in mice and to a
210 *Ceacam11*-like gene in the hamster. In addition, the N2 sequence of murine *Ceacam11-14* cluster
211 together with the N2 domain of the *Ceacam11*-like gene in the hamster. However, hamster C11-
212 like exons N1 and N2 do not exhibit clear orthology to any of the *Ceacam11-14* genes. Together,
213 this indicates that murine *Ceacam11-14* genes and the hamster *Ceacam11*-like gene have a
214 common ancestor (Fig. 4).



215
216 **Figure 4. Phylogenetic tree of *Ceacam/Psg*-related N domain nucleotide sequences of *Mus***
217 ***musculus* (house mouse) and *Cricetulus griseus* (Chinese hamster).** The phylogenetic tree was
218 constructed using the maximum likelihood (ML) method with bootstrap testing (500 replicates).
219 The bootstrap consensus tree inferred from 500 replicates is taken to represent the evolutionary
220 history of the exons analyzed. The percentage of replicate trees in which the associated exons
221 clustered together in the bootstrap test is shown next to the branches. Initial tree(s) for the
222 heuristic search were obtained automatically by applying Neighbor-Join and BioNJ algorithms to
223 a matrix of pairwise distances estimated using the Maximum Composite Likelihood (MCL)
224 approach, and then selecting the topology with superior log likelihood value. Multi-alignment of
225 N domain exon sequences was performed using Muscle implemented in MEGAX. For murine
226 *Psg31* and *Psg32* the name which is currently annotated in the NCBI and Ensemble databases are

227 indicated in brackets. Three letter code abbreviation for species: Mmu, *Mus musculus*; Cgr,
228 *Cricetulus griseus*.

229
230 Therefore, we used the nucleotide sequences of the *Ceacam11*-like gene in the hamster to search
231 for closely related N domain exons in other rodent species. With a few exceptions, we identified
232 one to four *Ceacam11*-like genes (composed of two N domain exons) in all species that also have
233 *Psg* and *Ceacam9* genes. A single *Ceacam11*-like gene was found in species of the Cricetidae,
234 Neotominae, and Deomyinae rodent subfamilies. In Murinae an amplification of the *Ceacam11*-
235 like gene had occurred, leading to two genes in rats, three genes in *Grammomys*, *Arvicanthis*, and
236 *Mastomys*, and four genes in the *Mus* genus (Fig. 2, Fig. 5). In Arvicolinae, only *Ceacam11*-like
237 gene remnants (N2 exons) could be identified. This indicates that this gene was lost in Arvicolinae.
238 Like in the *Psg* genes, orthologous relationship can only be observed in closely related rodent
239 species.



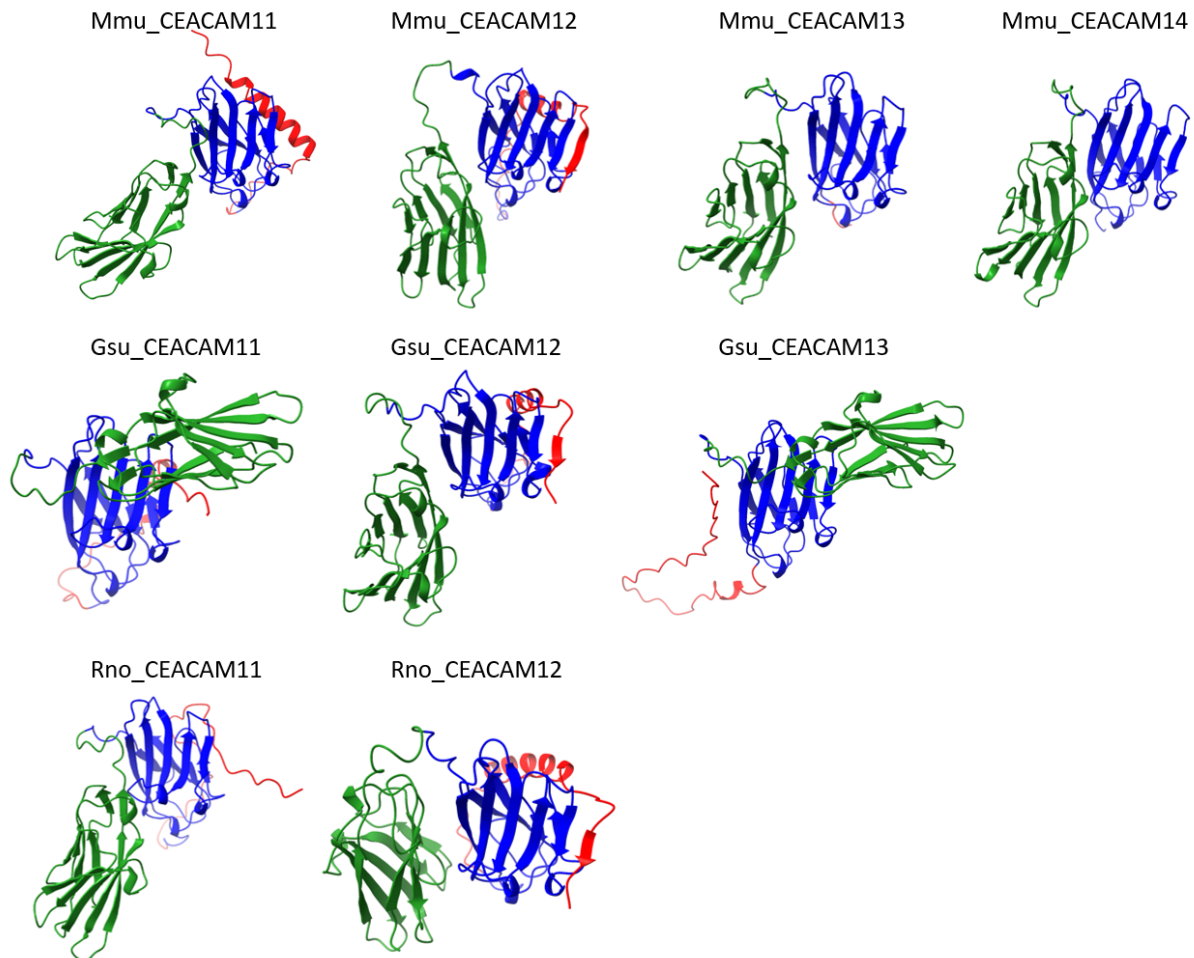
240
 241 **Figure 5: Phylogeny of the *Ceacam11-14* genes in rodents.** Nucleotide sequences complete
 242 coding sequence (A) the N1 exon (B) and the N2 exon (C) of the *Ceacam11-14* genes were used
 243 for phylogenetic analysis. The species abbreviations are explained in Fig. 1 and Supplementary
 244 Table 1. CC, Ceacam; P, indicates a missing open reading frame.

245

246 **Structure of rodent CEACAM11-14**

247 *Ceacam11-14* genes are in general composed of four exons with encode the leader sequence,
 248 the N1 domain and the N2 domain and a 3' exon harboring the stop codon. Murine *Ceacam14*

249 has a mutation in the splice donor site of exon 3 leading to the usage of a stop codon
250 immediately after the splice donor site. Interestingly, we could not identify exon 4 from rodents
251 with only 1 *Ceacam11*-like gene, however, the splice donor site of exon 3 is intact. Structurally,
252 *Ceacam12* is the most remarkable since the domain encoded by exon 4 is predicted to be part
253 of the ligand binding face of domain N2 which is formed by one of the two β -sheets present in
254 IgV-like domains. This structure is well conserved between different species, indicating that
255 there may exist a common ligand for CEACAM12 (Fig. 6).



256
257

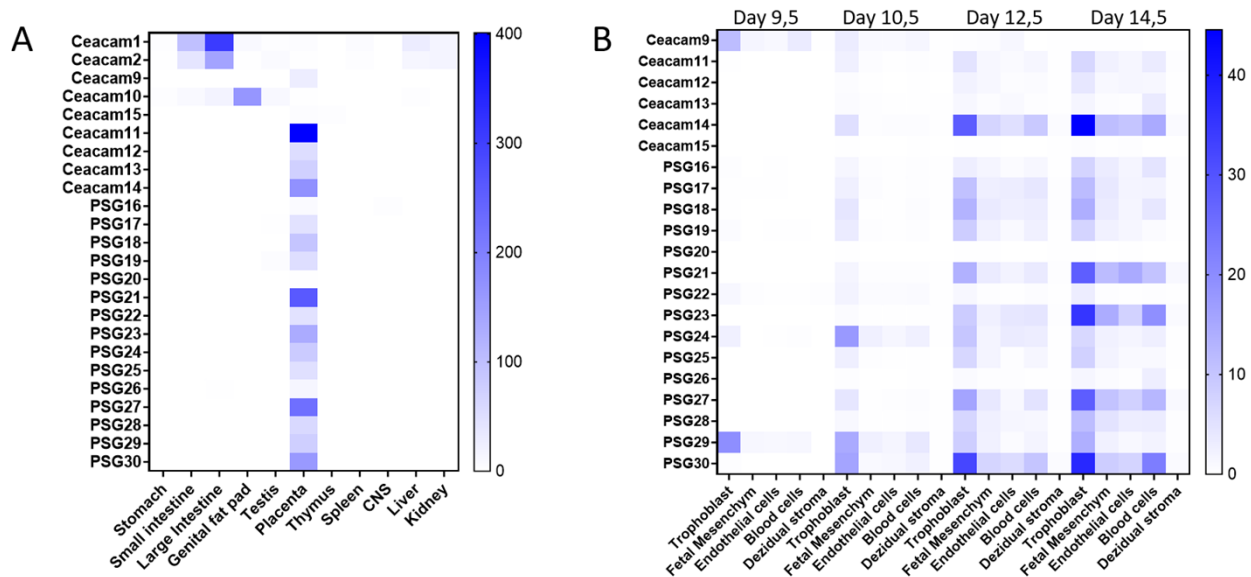
258 **Figure 6: Structure of the expanded CEACAM11-related CEACAMs.** The structure of the
259 CEACAM11-related CEACAMs from mouse (Mmu), African thickt rat (Gsu) and rat (Rno) was
260 predicted using ColabFold. The N1 domains are shown in green the N2 domains in blue and the
261 exon 4-encoded domain in red. The arrows represent β -strands.

262

263 ***Ceacam11-14* genes are preferentially expressed in trophoblast cells.**

264 PSGs are defined as CEACAM1-related CEACAMs that are secreted and preferentially expressed
265 in trophoblast cells [25]. Previously, we found that murine *Ceacam11-14* are expressed in
266 placental tissues in the mouse [7]. Here we substantiated these findings by additional analyses of

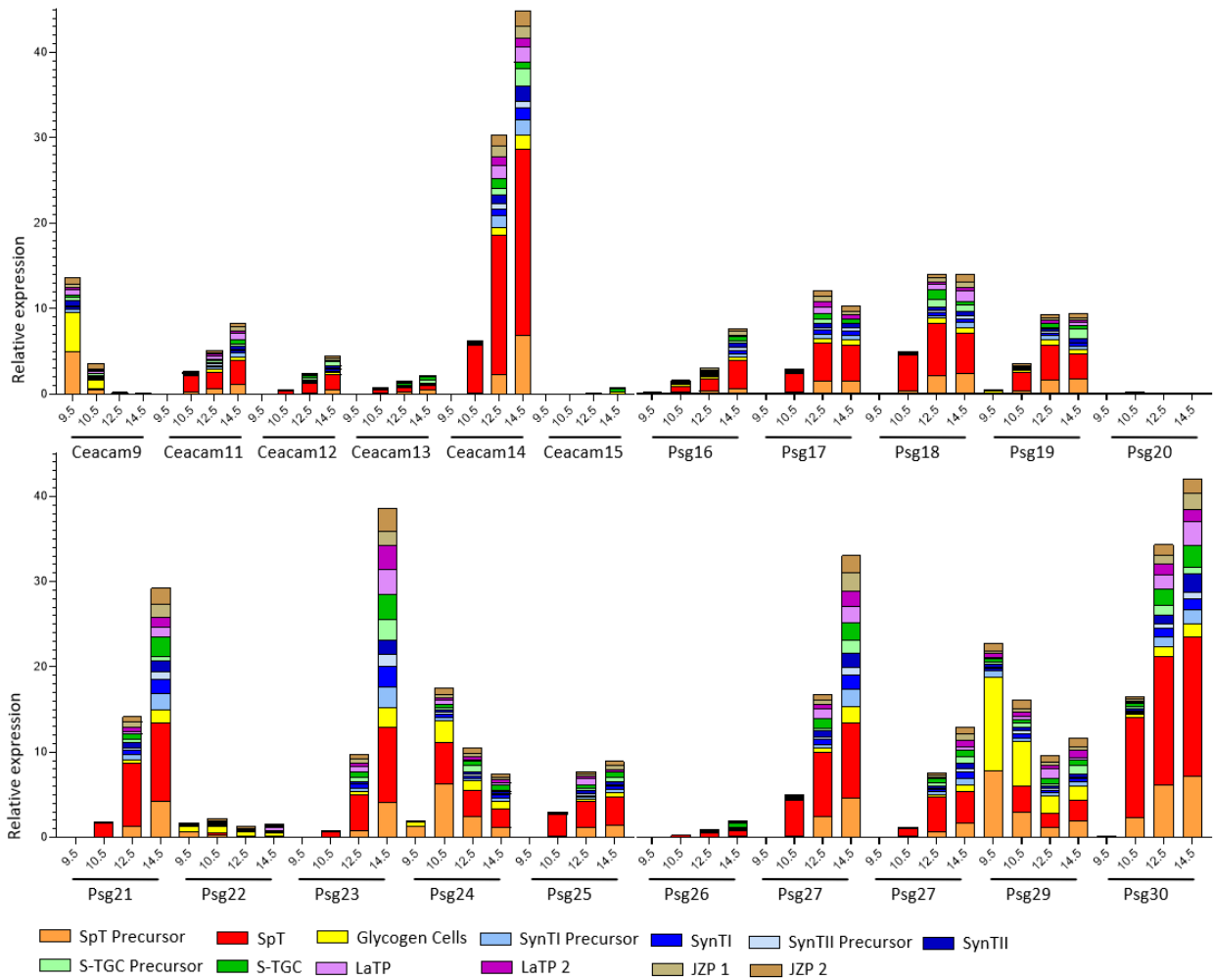
267 publicly available data sets as described in “Material and Methods”. Genes of the *Cea* gene family
 268 that were preferentially expressed in the placenta include *Ceacam9*, *Ceacam11-14*, and the *Psg*
 269 genes as determined by bulk mRNAseq data (Fig. 7A). scRNAseq data revealed that each of these
 270 genes is preferentially but not exclusively expressed by trophoblast cells in mice (Fig. 7B). In
 271 particular, *Ceacam14*, *Psg21*, *Psg23*, *Psg27*, and *Psg30* are expressed by additional tissue
 272 compartments in the placenta (Fig. 7B).
 273



274
 275
 276 **Figure 7: Expression of murine *Cea* gene family members.** (A) Expression of murine *Cea* gene
 277 family members in different tissues as extracted from the Mouse ENCODE project (NCBI Geo
 278 BioProject: PRJNA66167). The relative expression is based on bulk mRNAseq and indicated by the
 279 color code as depicted on the right. (B) Expression of placenta-specific *Cea* gene family members
 280 by different placental cell types as determined by scRNAseq [26]. The relative expression is
 281 indicated by the color code as depicted on the right.
 282

283 We further analyzed the expression of murine *Psgs* and *Psg-like Ceacams* by different trophoblast
 284 cell types at day 9.5, 10.5, 12.5 and 14.5 of pregnancy at single cell resolution. Overall murine
 285 *Psgs* and *Psg-like Ceacam* genes have a diverse expression pattern, although most genes were
 286 preferentially expressed by spongiotrophoblast cells and their precursors. However, in particular
 287 *Ceacam9* and *Psg29* were also expressed by glycogen cells. In addition, a significant expression of
 288 most *Psgs* and *Psg-like Ceacams* in syncytiotrophoblast cells and their precursors was noticed.
 289 *Psg23* showed the broadest expression pattern being expressed in different trophoblast cell
 290 types. *Ceacam15*, *Psg20*, *Psg22* and *Psg26* showed only a weak expression in placental cells at
 291 the investigated developmental stages. The expression of the majority of *Psgs* increased during
 292 pregnancy. In contrast, *Ceacam9* and *Psg29* showed the highest expression on day 9.5 followed

293 by a decrease of expression. *Psg24* reached a peak of expression on day 10.5 (Fig. 8). *Ceacam11-*
 294 *14* showed a very similar expression pattern although with significant differences of expression
 295 intensities at the mRNA level (Fig. 8). Together this expression analyses strongly indicate that all
 296 *Ceacam/Psg* genes at the “rodent *Psg* locus” have to be consider as functional *Psgs*.
 297



298
 299 **Figure 8: Relative expression of *Cea* gene family members in trophoblast subpopulations.** The
 300 color code that identifies the different cell populations is shown below the graph. SpT,
 301 Spongiotrophoblast; SynT1, outermost syncytiotrophoblast layer, SynT2, syncytiotrophoblast
 302 layer between SynT1 and the fetal endothelium; S-TGC, sinusoidal trophoblast giant cells; LaTP,
 303 labyrinth trophoblast progenitor; JZP, Junctional zone precursor [26].

304
 305 **The evolution of *Psgs* in Muroidea is highly dynamic**

306 Variation of *Psg* copy numbers within Muroidea indicates a highly dynamic evolution of *Psg* genes
 307 in the *Psg* gene locus. However, there are significant differences between groups of *Psg/Psg*-like
 308 *Ceacam* genes. *Ceacam9* and *Ceacam15* are well-conserved single-copy genes. *Ceacam9* is found
 309 in all *Psg*-containing species. In some closely related Muroidea species (*M. unguates*, *P. obesus*,

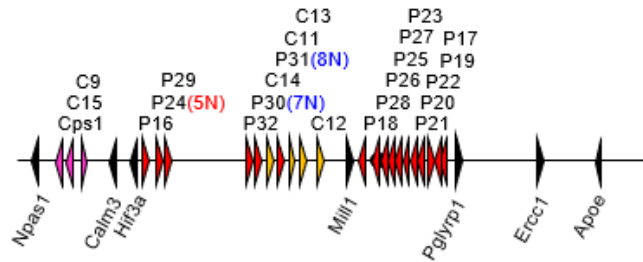
310 *R. opimus*) *Ceacam9* appears to be a pseudogene due to a common 2 bp deletion in the N exons
311 (Fig. 2; data not shown). In contrast, *Ceacam15* has been lost in the entire Arvicolinae subfamily
312 (only *Ceacam15* gene remnants can be found in some Arvicolinae species: Elu, Eta, Mgl, Ozi).
313 *Ceacam11* has been conserved for a certain time during which no amplification occurred. Only
314 recently this gene has been amplified in Murinae. The *bona fide* *Psg* genes have been subject to
315 multiple rounds of gene duplications and exon shuffling. Interestingly, gene expansion (possibly
316 followed by gene loss in some groups of species) happened differentially at different subregions
317 of the *Psg* locus of Muroidea species. While the number of *Psg*-like genes varies little in the *Psg*
318 subregion flanked by the marker genes *Hif3a* and *Mill1* (9-12 *Psg* and *Ceacam11-14* genes), there
319 is a large variation in *Psg* gene numbers in the *Psg* subregion flanked by *Mill1* and *Pglyrp1*, where
320 between 1 (*M. coucha*) and 11 *Psgs* (*M. musculus*) are found (Fig. 9). In contrast, most of *Psg* gene
321 size expansion by exon duplications occurred at the *Hif3a/Mill1* subregion (Fig. 9). Taken
322 together, this complex evolutionary history makes the assignment of orthologous genes almost
323 impossible between different families of Muroidea.

324

Murinae

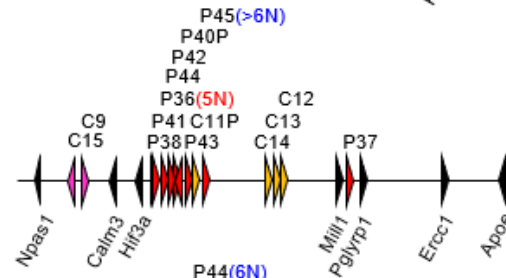
Mus musculus

House mouse
Chr 7 (GRCm39)



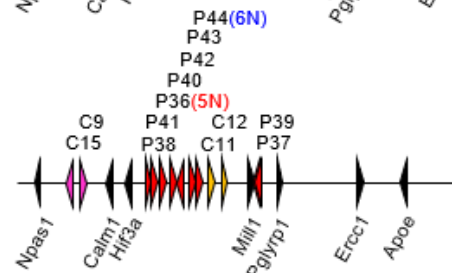
Mastomys coucha

Southern multimammate mouse
(VSBT01000021.1)



Rattus norvegicus

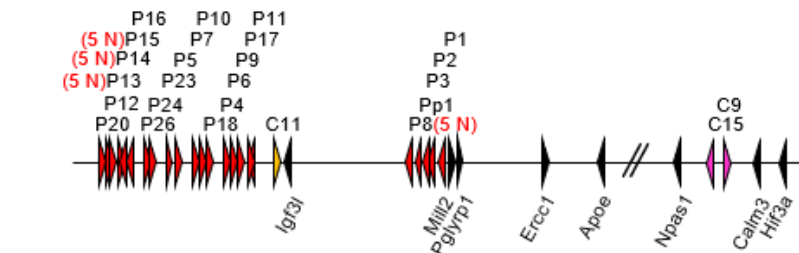
Norway rat
Chr 1 (mRatBN7.2)



Neotominae

Peromyscus maniculatus

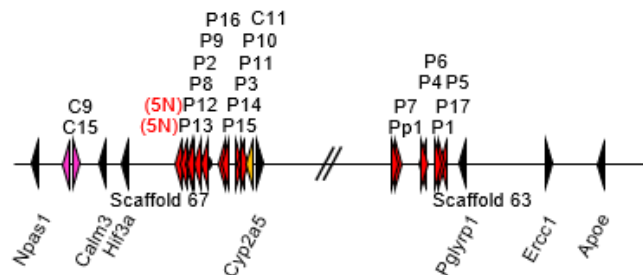
Northern American deer mouse
Primary_assembly_1



Cricetinae

Cricetulus griseus

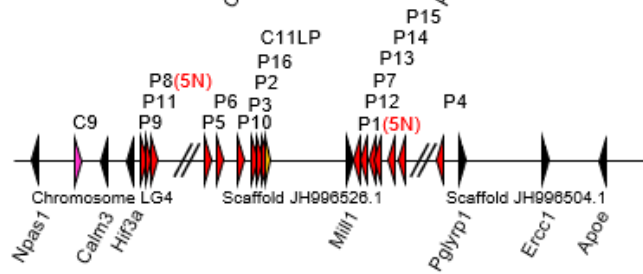
Chinese hamster
(CHOK1GS_HDV1)



Arvicolinae

Microtus ochrogaster

Prairie vole
(MicOch1.0)

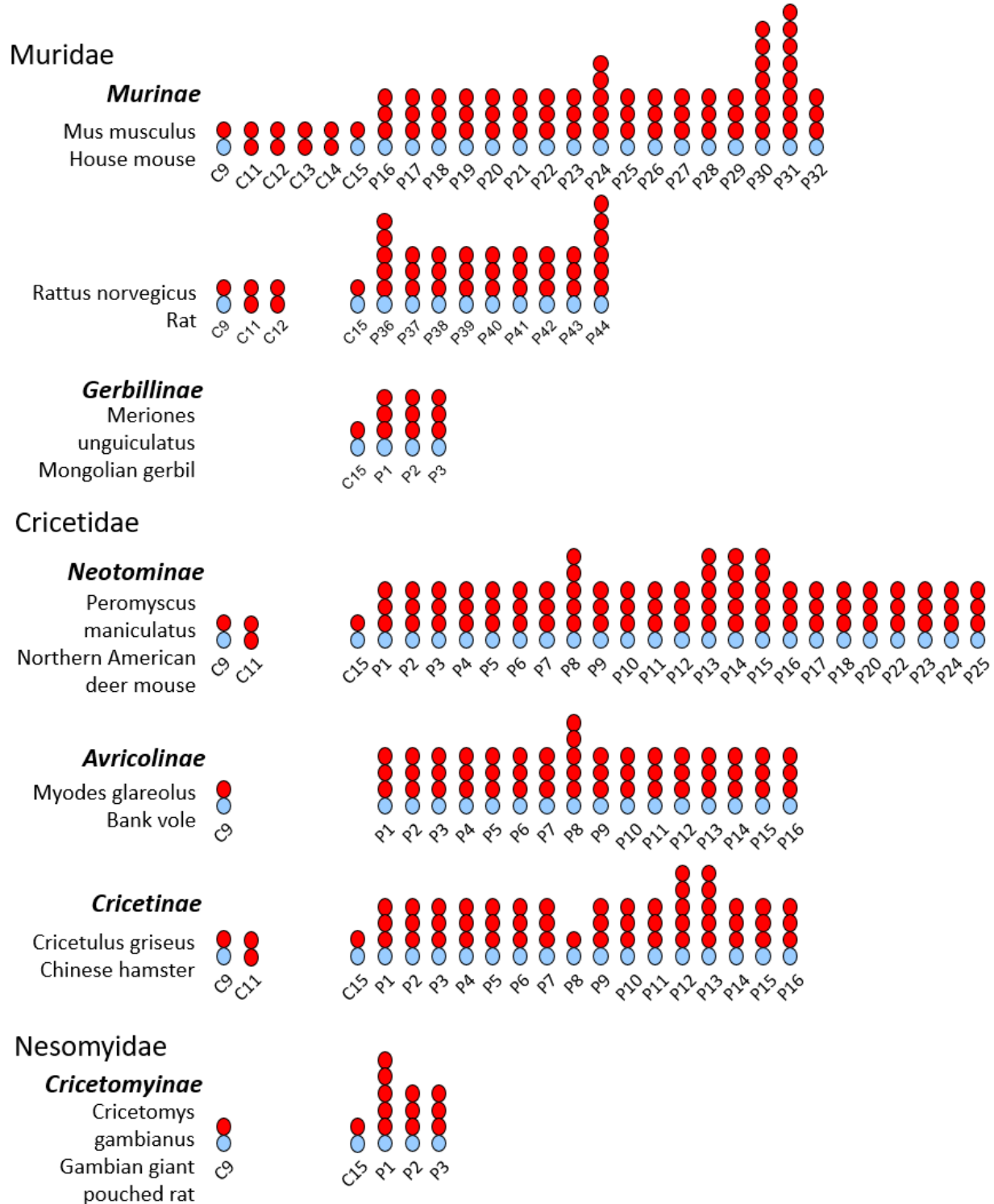


1 Mbp

327 **Figure 9. Divergent evolution of the *Psg* locus in Muroidea.** The chromosomal arrangements of
328 *Psg* genes at the *Npas1/Pglyrp1* locus of selected species of the Muroidea clade are shown.
329 Subfamily and species names are shown at the left side. Arrowheads indicate genes with their
330 transcriptional orientation. The *Psg*-related genes are shown in red (*Psg*), purple (*Ceacam9*,
331 *Ceacam15* and *Ceacam pseudogene 1*, *Cps1*) or orange (*Ceacam11-14*), and selected flanking
332 genes in black. The number of IgV domain-encoding exons exceeding the standard number 3 is
333 indicated in brackets next to the gene names. IgV variant order as found in Mmu_Psg24 and
334 Asp_Psg31 are shown in red and blue color, respectively. The *Psg* gene loci were aligned along
335 the position of the *Npas1* gene. Databases and their versions used are listed below the species
336 name. The borders of scaffolds are indicated by double slashes, their names below the
337 chromosome. Of note: ortholog assignment of *Ceacam11-14* genes between species is not
338 possible due to lack of unequivocal synteny and sequence relationship. Therefore, same gene
339 names do not imply an orthologous relationship. Asp, *Apodemus speciosus*; C, *Ceacam*; Cps,
340 *Ceacam pseudogene*; Mbp, million base pairs; Mmu, *Mus musculus*; P, pregnancy-specific
341 glycoprotein (*Psg*) genes.

342
343 **The structure of PSG/PSG-like CEACAMs in rodents**
344 Two principle domain compositions of PSGs/PSG-like CEACAMs were found in rodents, one group
345 consist of two N domains and the other is built by one A domain and a variable number of N
346 domains. Intact PSG-like CEACAMs built of two N domains are absent in various groups of rodents,
347 including Nesomyidae, Avricolinae, and Gerbillinae (Fig. 10). The dominant domain composition
348 of rodent PSGs is three N domains combined with one A domain (some 85 %), followed by PSGs
349 comprising five N domains and one A domain (Fig. 10). Nevertheless, in each species analyzed at
350 least one member is composed of one N domain and one A domain (Fig. 10).

351



352
353

354 **Figure 10: Domain structure of rodent PSGs/PSG-like CEACAMs.** The domain organization of
 355 PSG/PSG-like CEACAMs from selected rodent species from the Muridae, Cricetidae, and
 356 Nesomyidae families was predicted by gene analysis. Family, subfamily and species names are
 357 indicated at the left side. Mouse and rat PSG domain organizations were confirmed by EST
 358 sequences when available. IgV-like domains are shown as red, and IgC-like domains as blue ovals.

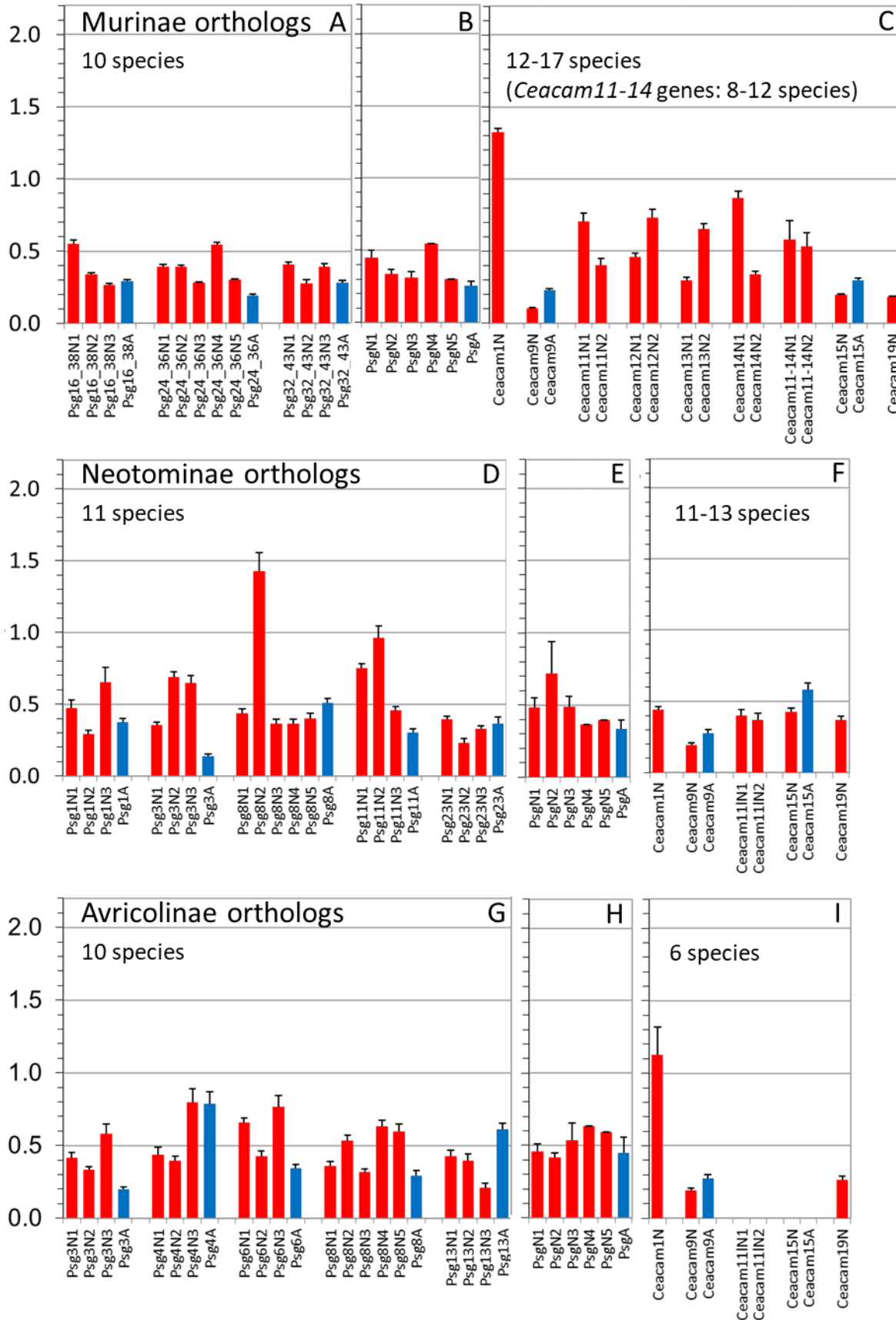
359 Note the highly variable number of PSG in the different rodent species (between 3 and 23).
360 Identical PSG numbering does not imply an orthologous relationship. C, CEACAM; P, PSG.

361

362 **Variable evolutionary selection on individual genes and rodent populations**

363 Previously we found that *PSGs* in bats after amplification are under selection for diversification.
364 In primates, we observed a largely variable selection pattern depending on the species and
365 domain examined. Here, we selected closely related groups of rodents where an orthologous
366 relationship between genes could be identified and performed dS/dN analyses. Three rodent
367 subfamilies could be analyzed Murinae, Neotominae, and Arvicolinae (Fig. 11). In all groups we
368 found that *Ceacam9* is highly conserved i.e., under purifying selection ($dN/dS < 1$) mostly even
369 more than the conserved *Ceacam19* gene (Fig 11 C, F, I). In contrast, the N domain of *Ceacam1* is
370 under selection for diversification (positive selection) in Murinae and Arvicolinae while it is under
371 purifying selection (negative selection) in Neotominae (Fig. 11 C, F, I) indicated by dN/dS values
372 >1 and <1 , respectively. Remarkably, the positive selection of the *Ceacam1* N domain exon in
373 Murinae as in other species (e.g. humans) is thought to be the result of pathogen usage of
374 CEACAM1 as an entry receptor. In general, PSGs in rodents are under negative selection (Fig. 11
375 A, B, D, E, G, H). In Neotominae and Arvicolinae individual N domains and A domains show a
376 relaxation of negative selection. In particular, the N2 domains of PSG8 and PSG11 in Neotominae
377 exhibit or are close to positive selection, respectively. In Arvicolinae several N and A domain exons
378 show a relaxed negative selection ($0.5 < dN/dS < 1.0$) (Fig. 11 G, H). The single *CEACAM11-14* gene
379 in Neotominae is under negative selection ($dN/dS = \sim 0.4$), in contrast in Murinae the *Ceacam11-*
380 *14* genes show some relaxation of purifying selection, indicating that upon amplification the
381 newly generated genes underwent some adaptation to their new functions Fig. 11 C.

382



384 **Figure 11. Differential selection for diversification in Ig domain exons of trophoblast-specific**
385 ***Ceacam/Psg* genes.** Nucleotide sequences of N and A domain exons of *Psg* orthologs from rodent
386 species A-C: Murinae (Ani, Asy, Gsu, Hal, Mca, Mco, Mmi, Mmu, Mmu_cas, Mmu_mus, Mna, Mpa,
387 Msi, Msp, Pde, Rdi, Rno, Rra), D: Neotominae (Nle, Oto, Pat, Paz, Pca, Per, Ple, Pma, Pme, Pnu,
388 Ppo) and G: Arvicolinae subfamilies (Elu, Eta, Mag, Mar, Mfo, Mgl, Moc, Moe, Mor, Ozi) were
389 compared pair-wise in all combinations after manual removal of gaps and the ratio of the rate of
390 nonsynonymous (dN) and synonymous mutations (dS) was calculated for whole N and A domain
391 exons and the mean ratios were plotted. The whiskers represent standard errors of the mean
392 (SEM). Only genes were included for which an orthologous relationship could be demonstrated
393 by phylogenetic analyses using CLUSTALW. The dN/dS values of three to five PSG genes for each
394 exon type and subfamily were averaged and plotted (B, E, H). In addition, the dN/dS ratios for the
395 N domain exons of trophoblast-specific *Ceacam* genes and, for comparison, for *Ceacam1* and
396 *Ceacam19* orthologs of the same rodent species were calculated (C, F, I). These two genes are
397 known to represent genes under diversifying (dN/dS > 1) and purifying selection (dN/dS <<1),
398 respectively, in other mammalian species [23]. Of note: In Neotominae species, for the single
399 gene related to the CEACAM11-14 genes in Murinae no ortholog could be clearly identified. A,
400 IgC-like domain exon; N, N domain exon; CEACAM11L, CEACAM11-like. For the three letter
401 species name abbreviations please refer to Supplementary Table 1.

402
403 **Independent evolution of *Psgs* in rodents without a “rodent *Psg* locus”?**
404 Since structurally different *Psgs* evolved in Muroidea it is worth speculating that in other rodents
405 *Psgs* evolved at a different locus in the genome as found for Muroidea. Indeed, we found some
406 amplification of *Ceacams* at the *Ceacam* locus flanked by the marker genes *Cd79a* and *Xrcc1*.
407 However, there is no evidence that these genes represent *bona fide* genes that encode secreted
408 proteins or are expressed in a trophoblast-specific manner. In contrast, in species where we
409 further analyzed the expanded *Ceacams* we found also an expansion of transmembrane domain
410 coding exons, suggesting that these are membrane-bound *Ceacams*. Nevertheless, since
411 expression data are lacking we cannot exclude that *Psgs* evolved in other rodents than the ones
412 described in the present report.

413
414 **Discussion**
415 *PSGs* were so far described in primates, mice and rats, microbats, and the horse [9, 14, 16]. With
416 the exception of the horse, these species have a hemochorial placenta. Thus, we have previously
417 speculated that the intimate contact of trophoblast cells with maternal immune cells drives the
418 evolution of *PSGs* [11, 16, 23]. Indeed, in primates, the emergence of *PSGs* correlates with the
419 appearance of hemochorial placentation [16]. The only primates so far identified that have a
420 hemochorial placenta but no *PSGs* are the tarsiers [16] indicating that in primates *PSGs* evolve
421 almost in parallel to a hemochorial type of placentation. However, while the amplification of *PSG*
422 genes in New World monkeys remained limited (1-7 *PSG* genes) a massive amplification occurred

423 in Old World monkeys resulting in more than 20 gene copies in some species [16]. These
424 differences may be due to unknown restrictions of successful gene duplication at the *PSG* locus
425 in New World monkeys or by a relaxed selection pressure for *PSG* gene amplification. In order to
426 get further insights into the evolution of *PSG* genes we analyzed the evolution of *Psgs* in rodents.
427 Since all rodents, with very few exceptions, have a hemochorial placenta we expected that in
428 most if not all rodents *Psgs* are present, although they have been only described in mice and rats
429 so far. It has been suggested that the common ancestor of rodents had a hemochorial
430 placentation with an interhemal barrier that had a single layer of syncytial trophoblast cells [18].
431 This anatomical feature was retained in the clade comprising Hystricomorpha (guinea pigs and
432 others) and Sciuromorpha (squirrels) [18]. In contrast, in Myomorpha (mice and others) several
433 placental transformations occurred [18], most remarkably within the Muridae family, which has
434 a special three-layered trophoblast [27, 28]. The three-layered trophoblast containing a layer of
435 cytotrophoblast and two layers of syncytiotrophoblast cells appeared together with the capture
436 of the *syncytin-A* and *syncytin-B* genes in the most recent common ancestor (MRCA) of Muroidea
437 including Muridae, Cricetidae, and Spalacidae family species [29]. Of them, the Spalacidae is the
438 only family in which *Psgs* did not evolve indicating that shortly after the invention of the three-
439 layered trophoblast *Psgs* evolved. This may refine our picture of the forces driving PSG
440 development. It may be that alterations of the fetomaternal interface create opportunities to
441 optimize the molecular fetomaternal crosstalk. Members of the CEA family may be predisposed
442 to fulfill this task once they are secreted by fetal trophoblast cells. Such a “beneficial” *PSG* gene
443 may then be fixed in the genome and eventually amplified. Because the fetomaternal interface
444 evolves extraordinarily fast such changes may frequently occur thus explaining why PSGs can
445 evolve independently multiple times in different mammalian lineages. Since *Ceacam9*,
446 *Ceacam15*, and *Ceacam11-like* genes or at least remnants of the latter are present in the genome
447 of *Psg*-harboring rodents it is not possible to decide which ancestor of these genes is the
448 primordial gene of rodent *Psgs*. However, a combination of *Ceacam9* or *Ceacam15* with
449 *Ceacam11-14* would provide all building blocks (three N domain exons and one A domain exon)
450 to create typical rodent *Psgs*. The strong correlation between the existence of *Psgs* and the
451 presents of *Ceacam9* may indicate that *Ceacam9* plays a pivotal role in the evolution of *Psg* genes.
452 If *Ceacam9* is the founder of *Psgs*, *Ceacam15* may be an early duplicate of *Ceacam9* which gained
453 a new function but was not further amplified. The high conservation of *Ceacam15* argues for such
454 a speculation. On the other hand, *Ceacam15* and the ancestor of *Ceacam11-14* were lost in
455 Arvicolinae indicating that in the MRCA of this group, both genes lost their function and therefore
456 were subsequently deleted from the genome. Rodent PSGs are in general composed of three
457 (more rarely of five, six, seven or eight) IgV-like domains and one A domain of the A2 type. Since
458 the vast majority of rodent PSGs are composed of the typical exon arrangement with 3 exons
459 coding for IgV-like domains and one IgC-like domain we conclude that once a *Psg* gene had
460 evolved the duplication of whole *Psg* genes was the major mechanism of *Psg* gene amplification
461 in rodents. The expansion of PSGs is still ongoing as indicated by the different number of *Psg*

462 genes and their independent expansion e.g. in mice and rats. In addition, as previously shown for
463 mouse *Psgs*, *Psgs* of other Muroidea evolve extremely fast therefore orthologs can only be
464 assigned between very closely related species (Fig. 4) [24]. The fast evolution limits the possibility
465 to analyze the nature of selection on rodent *Psgs* (Fig. 11). Nevertheless, our results indicate that
466 some PSGs in some species are under positive selection, but the majority are under purifying
467 selection. These results suggest that most rodent PSGs have adapted to a certain function while
468 only some, possibly newly duplicated, PSGs are free to acquire novel functions or ligands. More
469 recently, a second wave of gene amplification took place. The ancestor of *Ceacam11-14* is under
470 purifying selection in all species that have only one gene. In Murinae the purifying selection seems
471 to be relaxed, enabling some flexibility for functional optimization (Fig. 11). Remarkably,
472 CEACAM11-14 are structurally different from the bona fide PSGs in rodents composed of only one
473 N domain and one A domain. However, the very similar expression pattern of *Ceacam11-14* and
474 *Psgs* in placental cells (Fig. 7; Fig. 8; [30]) suggest that both are functional “PSGs”. We have
475 previously reported that PSGs are structurally different in different species, due to an
476 independent evolution. This is now the first report showing that PSGs did evolve twice in one
477 mammalian group, leading to structurally distinct PSGs. This indicates that the birth of PSGs is a
478 frequent event explaining the independent evolution in various mammalian lineages.

479 Since the translocation of a *Ceacam* gene family member or parts of it seem to be a hallmark of
480 the evolution of *Psgs* in rodents the question arises what kind of *Ceacam* gene was translocated
481 to form the original *Psg* locus? One possibility can be envisaged that part of an ITAM-containing
482 *Ceacam* gene was translocated with concomitant destruction/loss of the ITAM motif-encoding
483 region of the gene. Such a scenario would explain the strong correlation between the absence of
484 ITAM-containing CEACAMs and the presence of PSGs (Fig. 3). In rodents without PSGs, ITAM-
485 containing CEACAMs exist, as in most other mammalian species (Fig. 3) [23]. Thus, this report
486 shows for the first time that most rodents have ITAM-harboring CEACAMs and that the loss of
487 ITAM-containing CEACAMs happened only recently affecting the species of the Muridae family. A
488 summary of the possible evolution of *Psgs* in rodents is depicted in Supplementary Figure 2.

489 Although we did not find any evidence for the presence of PSG in other rodents we cannot exclude
490 that they may exist in some species due to their structural variability and missing expression data
491 of most species analyzed in this report. In addition, we are aware that the simplified construction
492 of rodent phylogeny used in this study by comparing the IgV-like (N) domain exons of *CEACAM19*
493 did not completely mirror the previously published studies using more complex molecular data
494 [21, 22, 31]. In contrast to these studies, we did not see a monophyletic clade comprising
495 Hystricomorpha and Sciuromorpha. In addition, the Castorimorpha did not appear to be a sister
496 group of the Myomorpha as previously shown. Nevertheless, the relationship between the
497 Muridae and Dipodidae as well as the relationship within the Muridae family agrees with
498 published data [21, 22, 31].

499 In summary, the expansion of the analysis of the CEA gene family to the entire rodent clade shed
500 new light on the evolution of the CEA gene family of the most frequently used animal models for

501 medical research, i.e. mice and rats. This study demonstrates that the loss of an ITAM-encoding
502 *Ceacam* gene and the appearance of *Psg* genes is a rather recent event in rodents only affecting
503 the Cricetidae, Muridae and Nesomyidae families.

504

505 **Methods**

506 **Identification and nomenclature of genes**

507 Nucleotide and amino acid sequence searches were performed using the NCBI BLASTBLAT tools
508 (<http://www.ncbi.nlm.nih.gov/BLAST>) and the Ensembl database
509 (<http://www.ensembl.org/Multi/Tools/Blast?db=core>) using default parameters. For the
510 identification of rodent *Ceacam* exons, *Ceacam* and *Psg* exon and cDNA sequences from known
511 mouse and rat *Ceacam/Psgs* were used to search various databases at NCBI and Ensembl
512 including whole-genome shotgun contigs (wgs), and Transcriptome Shotgun Assembly (TSA). A
513 comprehensive overview of the used genomic data sources for the analyzed rodent species is
514 given in Supplementary Table 1. Hits were considered to be significant if the E-value was $< e^{-10}$
515 and the query cover was $> 50\%$. Genes that contained stop codons within their N domain exons
516 or lacked appropriate splice acceptor and donor sites in these exons were considered to represent
517 pseudogenes. Nucleotide sequences from the N domain exons can be used as gene identifiers
518 (Supplementary File 2). The same strategy was employed to identify other genes of the CEACAM
519 families. *Ceacam* genes, the N exons of which exhibited $>99\%$ nucleotide sequence identity, were
520 considered to represent alleles.

521

522 **Quantification of PSG expression**

523 For the quantification of murine PSG expression, we reanalyzed publicly available datasets, these
524 include mRNA sequencing data sets generated by the Mouse ENCODE project available at NCBI
525 Geo BioProject: PRJNA66167 as well as single cell mRNA sequencing data available at
526 [https://figshare.com/projects/Single_nuclei_RNA-](https://figshare.com/projects/Single_nuclei_RNA-seq_of_mouse_placental_labyrinth_development/92354)
527 [seq_of_mouse_placental_labyrinth_development/92354](https://figshare.com/projects/Single_nuclei_RNA-seq_of_mouse_placental_labyrinth_development/92354) [26, 32].

528

529 **Sequence motif identification and 3D modeling**

530 The presence of immunoreceptor tyrosine-based activation motifs (ITAM), ITAM-like, and
531 immunoreceptor tyrosine-based inhibition motifs (ITIM) and immunoreceptor tyrosine-based
532 switch motifs (ITSM) were confirmed using the amino acid sequence pattern search program ELM
533 (<http://elm.eu.org/>). Transmembrane regions, and leader peptide sequences were identified
534 using the TMHMM (<http://www.cbs.dtu.dk/services/TMHMM-2.0/>), the SignalP 4.1 programs
535 (<http://www.cbs.dtu.dk/services/SignalP/>), respectively. The structure predictions of murine
536 CEACAM11-14 and rat CEACAM11-12 were retrieved from the “AlphaFold Protein Structure
537 Database”. The structure of CEACAM11-13 from African tree rat (*Grammomys surdaster*) was
538 predicted using “ColabFold” [33].

539

540 **Phylogenetic analyses and determination of positive and purifying selection**

541 Phylogenetic analyses based on nucleotide and amino acid sequences were conducted using
542 MEGAX [34]. Sequence alignments were performed using Muscle implemented in MEGAX.
543 Phylogenetic trees were constructed using the maximum likelihood (ML) method with bootstrap
544 testing (500 replicates) and the Tamura-Nei substitution model [35]. Other multiple sequence
545 alignments were performed with CLUSTALW programs ([http://npsa-pbil.ibcp.fr/cgi-](http://npsa-pbil.ibcp.fr/cgi-bin/npsa_automat.pl?page=/NPSA/npsa_clustalw.html)
546 [bin/npsa_automat.pl?page=/NPSA/npsa_clustalw.html](http://npsa-pbil.ibcp.fr/cgi-bin/npsa_automat.pl?page=/NPSA/npsa_clustalw.html);
547 <http://www.genome.jp/tools/clustalw/>). In order to determine the selective pressure on the
548 maintenance of the nucleotide sequences, the number of nonsynonymous nucleotide
549 substitution per nonsynonymous site (dN) and the number of synonymous substitutions per
550 synonymous site (dS) were determined for *Psg* and *Ceacam* N domain and IgC-like exons. The
551 dN/dS ratios between pairs of *Psg* orthologs and paralogs and orthologous *Ceacam* genes were
552 calculated after manual editing of sequence gaps or insertions guided by the amino acid
553 sequences using the SNAP program (Synonymous Nonsynonymous Analysis Program;
554 <http://www.hiv.lanl.gov/content/sequence/SNAP/SNAP.html>) [36].

555

556 **Declarations**

557 **Ethics approval and consent to participate**

558 Not applicable

559

560 **Consent for publication**

561 Not applicable

562

563 **Availability of data and materials**

564 All relevant data are publicly available and described in the manuscript

565

566 **Competing interests**

567 The authors declare that they have no competing interests

568

569 **Funding**

570 There was no specific funding source for this work

571

572 **Authors' Contributions**

573 R.K. conceived the study, carried out data analysis and drafted the manuscript. W.Z. performed
574 most of the data mining and contributed equally to manuscript writing. Both authors read and
575 approved the final manuscript.

576

577 **Acknowledgements**

578 Not applicable

579 **References**

- 580 1. Bohn H: **[Detection and characterization of pregnancy proteins in the human placenta and**
581 **their quantitative immunochemical determination in sera from pregnant women]**. *Archiv fur*
582 *Gynakologie* 1971, **210**(4):440-457.
- 583 2. Oikawa S, Inuzuka C, Kosaki G, Nakazato H: **Exon-intron organization of a gene for pregnancy-**
584 **specific beta 1-glycoprotein, a subfamily member of CEA family: implications for its**
585 **characteristic repetitive domains and C-terminal sequences**. *Biochemical and biophysical*
586 *research communications* 1988, **156**(1):68-77.
- 587 3. Streydio C, Lacka K, Swillens S, Vassart G: **The human pregnancy-specific beta 1-glycoprotein (PS**
588 **beta G) and the carcinoembryonic antigen (CEA)-related proteins are members of the same**
589 **multigene family**. *Biochemical and biophysical research communications* 1988, **154**(1):130-137.
- 590 4. Chan WY, Tease LA, Bates JM, Jr., Borjigin J, Shupert WL: **Pregnancy-specific beta 1 glycoprotein**
591 **in rat: tissue distribution of the mRNA and identification of testicular cDNA clones**. *Hum*
592 *Reprod* 1988, **3**(5):687-692.
- 593 5. Ogilvie S, Shiverick KT, Larkin LH, Romrell LJ, Shupert WL, Chan WY: **Pregnancy-specific beta 1-**
594 **glycoprotein messenger ribonucleic acid and immunoreactive protein in the rat testis**.
595 *Endocrinology* 1990, **126**(1):292-298.
- 596 6. Rudert F, Saunders AM, Rebstock S, Thompson JA, Zimmermann W: **Characterization of murine**
597 **carcinoembryonic antigen gene family members**. *Mammalian genome : official journal of the*
598 *International Mammalian Genome Society* 1992, **3**(5):262-273.
- 599 7. Zebhauser R, Kammerer R, Eisenried A, McLellan A, Moore T, Zimmermann W: **Identification of a**
600 **novel group of evolutionarily conserved members within the rapidly diverging murine Cea**
601 **family**. *Genomics* 2005, **86**(5):566-580.
- 602 8. Kammerer R, Mansfeld M, Hanske J, Missbach S, He X, Kollner B, Mouchantat S, Zimmermann W: **Recent**
603 **expansion and adaptive evolution of the carcinoembryonic antigen family in bats of the**
604 **Yangochiroptera subgroup**. *BMC genomics* 2017, **18**(1):717.
- 605 9. Aleksic D, Blaschke L, Missbach S, Hanske J, Weiss W, Handler J, Zimmermann W, Cabrera-Sharp
606 V, Read JE, de Mestre AM *et al*: **Convergent evolution of pregnancy-specific glycoproteins in the**
607 **human and horse**. *Reproduction* 2016.
- 608 10. Ballesteros A, Mentink-Kane MM, Warren J, Kaplan GG, Dveksler GS: **Induction and activation of**
609 **latent transforming growth factor-beta1 are carried out by two distinct domains of pregnancy-**
610 **specific glycoprotein 1 (PSG1)**. *The Journal of biological chemistry* 2015, **290**(7):4422-4431.
- 611 11. Kammerer R, Ballesteros A, Bonsor D, Warren J, Williams JM, Moore T, Dveksler G: **Equine**
612 **pregnancy-specific glycoprotein CEACAM49 secreted by endometrial cup cells activates TGFB**.
613 *Reproduction* 2020, **160**(5):685-694.
- 614 12. Martinez FF, Cervi L, Knubel CP, Panzetta-Dutari GM, Motran CC: **The role of pregnancy-specific**
615 **glycoprotein 1a (PSG1a) in regulating the innate and adaptive immune response**. *American*
616 *journal of reproductive immunology* 2013, **69**(4):383-394.
- 617 13. Warren J, Im M, Ballesteros A, Ha C, Moore T, Lambert F, Lucas S, Hinz B, Dveksler G: **Activation**
618 **of latent transforming growth factor-beta1, a conserved function for pregnancy-specific beta**
619 **1-glycoproteins**. *Mol Hum Reprod* 2018, **24**(12):602-612.
- 620 14. Moore T, Williams JM, Becerra-Rodriguez MA, Dunne M, Kammerer R, Dveksler G: **Pregnancy-**
621 **specific glycoproteins: evolution, expression, functions and disease associations**. *Reproduction*
622 *2022*, **163**(2):R11-R23.
- 623 15. Moore T, Dveksler GS: **Pregnancy-specific glycoproteins: complex gene families regulating**
624 **maternal-fetal interactions**. *The International journal of developmental biology* 2014, **58**(2-
625 4):273-280.

- 626 16. Zimmermann W, Kammerer R: **The immune-modulating pregnancy-specific glycoproteins**
627 **evolve rapidly and their presence correlates with hemochorial placentation in primates.** *BMC*
628 *genomics* 2021, **22**(1):128.
- 629 17. Lunn P, Vagnoni KE, Ginther OJ: **The equine immune response to endometrial cups.** *Journal of*
630 *reproductive immunology* 1997, **34**(3):203-216.
- 631 18. Mess AM, Carter AM: **Evolution of the interhaemal barrier in the placenta of rodents.** *Placenta*
632 2009, **30**(10):914-918.
- 633 19. Meng J, Wyss AR, Dawson MR, Zhai R: **Primitive fossil rodent from Inner Mongolia and its**
634 **implications for mammalian phylogeny.** *Nature* 1994, **370**(6485):134-136.
- 635 20. Connor J Burgin JPC, Philip L Kahn, Nathan S Upham: **How many species of mammals are there?**
636 *Journal of Mammalogy*, 2018, **99** (1):1–14.
- 637 21. Fabre PH, Hautier L, Dimitrov D, Douzery EJ: **A glimpse on the pattern of rodent diversification:**
638 **a phylogenetic approach.** *BMC evolutionary biology* 2012, **12**:88.
- 639 22. Steppan S, Adkins R, Anderson J: **Phylogeny and divergence-date estimates of rapid radiations**
640 **in muroid rodents based on multiple nuclear genes.** *Syst Biol* 2004, **53**(4):533-553.
- 641 23. Kammerer R, Zimmermann W: **Coevolution of activating and inhibitory receptors within**
642 **mammalian carcinoembryonic antigen families.** *BMC biology* 2010, **8**:12.
- 643 24. McLellan AS, Fischer B, Dveksler G, Hori T, Wynne F, Ball M, Okumura K, Moore T, Zimmermann
644 W: **Structure and evolution of the mouse pregnancy-specific glycoprotein (Psg) gene locus.**
645 *BMC genomics* 2005, **6**:4.
- 646 25. Kammerer R, Herse, F., Zimmermann, W.: **Convergent Evolution Within CEA Gene Families in**
647 **Mammals: Hints for Species-Specific Selection Pressures.** Berlin: Springer; 2016.
- 648 26. Marsh B, Blelloch R: **Single nuclei RNA-seq of mouse placental labyrinth development.** *Elife*
649 2020, **9**.
- 650 27. Enders AC: **A Comparative Study of the Fine Structure of the Trophoblast in Several**
651 **Hemochorial Placentas.** *Am J Anat* 1965, **116**:29-67.
- 652 28. King BF, Hastings RA, 2nd: **The comparative fine structure of the interhemal membrane of**
653 **chorioallantoic placentas from six genera of myomorph rodents.** *Am J Anat* 1977, **149**(2):165-
654 179.
- 655 29. Vernochet C, Redelsperger F, Harper F, Souquere S, Catzeflis F, Pierron G, Nevo E, Heidmann T,
656 Dupressoir A: **The captured retroviral envelope syncytin-A and syncytin-B genes are conserved**
657 **in the Spalacidae together with hemotrichorial placentation.** *Biology of reproduction* 2014,
658 **91**(6):148.
- 659 30. Green MT, Martin RE, Kinkade JA, Schmidt RR, Bivens NJ, Tuteja G, Mao J, Rosenfeld CS:
660 **Maternal oxycodone treatment causes pathophysiological changes in the mouse placenta.**
661 *Placenta* 2020, **100**:96-110.
- 662 31. Swanson MT, Oliveros CH, Esselstyn JA: **A phylogenomic rodent tree reveals the repeated**
663 **evolution of masseter architectures.** *Proceedings Biological sciences* 2019, **286**(1902):20190672.
- 664 32. Davis CA, Hitz BC, Sloan CA, Chan ET, Davidson JM, Gabdank I, Hilton JA, Jain K, Baymuradov UK,
665 Narayanan AK *et al*: **The Encyclopedia of DNA elements (ENCODE): data portal update.** *Nucleic*
666 *acids research* 2018, **46**(D1):D794-D801.
- 667 33. Mirdita M, Schutze K, Moriwaki Y, Heo L, Ovchinnikov S, Steinegger M: **ColabFold: making**
668 **protein folding accessible to all.** *Nat Methods* 2022, **19**(6):679-682.
- 669 34. Kumar S, Stecher G, Li M, Knyaz C, Tamura K: **MEGA X: Molecular Evolutionary Genetics Analysis**
670 **across Computing Platforms.** *Molecular biology and evolution* 2018, **35**(6):1547-1549.
- 671 35. Tamura K, Nei M: **Estimation of the number of nucleotide substitutions in the control region of**
672 **mitochondrial DNA in humans and chimpanzees.** *Molecular biology and evolution* 1993,
673 **10**(3):512-526.

- 674 36. B. K: **HIV Signature and Sequence Variation Analysis. Computational Analysis of HIV Molecular**
675 **Sequences.** Dordrecht, Netherlands: Kluwer Academic Publishers; 2000.
676